Summer Bioengineering Conference
SBC2025
June 22-25, 2025, Santa Ana Pueblo, New Mexico, USA

CORTICAL CURVEDNESS PATTERNS ALTER WITH VOLUMETRIC EXPANSION DURING INFANCY: A LONGITUDINAL ANALYSIS

C. Godin (1), M. Holland (1,2)

(1) Bioengineering Graduate Program, University of Notre Dame, Notre Dame, IN, USA
(2) Department of Aerospace & Mechanical Engineering, University of Notre Dame, Notre Dame, IN, USA

INTRODUCTION

The brain's outermost layer, the cerebral cortex, is responsible for the sense-perception, memory, and decision making at the focal point of the human conscious experience. In humans, the cortex starts to expand volumetrically during the second trimester of pregnancy, where genetic actors and cellular mechanisms work to maximize surface area within the constraints of the skull [1]. Rapid radial expansion, preferential variation in growth rates, cell-density gradients, stiffness ratios, and axonal forces lead to buckling in which characteristic gyri (hills) and sulci (valleys) are formed. This phenomenon, known as gyrification, has yet to be fully elucidated; a combination of both biological and mechanical factors likely contribute to the cortex's shape achieved by early adulthood [2]. Through computational modeling, researchers have made significant progress in describing observed curvature and thickness variations throughout the cortex, where describing these growth patterns highlights typical and atypical biomarkers of neurological development that may help predict the presence or risk of various disease states.

The nuances of folding, curvature, and thickness patterns certainly affect neural functionality, where maximizing cortical surface area efficiently increases cognitive capacity. Systematic differences, like thick gyri and thin sulci, are likely the result of engineering phenomena which play a concerted role [3]. For example, our group has modeled how gyral–sulcal thickness variations are a low-stiffness-ratio phenomenon, where inhomogeneous cortical growth is likely a result of folding rather than the cause [4]. These variations are further influenced by mechanical stresses during folding, as compressive forces thicken gyri while tensile forces thin sulci [5]. We have also mapped cortical morphology across neonates, adults, and non-human primates to better understand the distribution of cortical thickness patterns [6-8].

We use MRI data to computationally analyze the cortex, linking basic measures such as thickness to curvature metrics like shape index to gain insights into the brain's folding patterns. Here we introduce our computational pipeline in a longitudinal cohort of infants for the first time. Not only does this fill in a portion of our timeline previously left unexplored, but images of the same subject brain throughout infancy gives greater insight into how certain curvature metrics, along with thickness, dynamically change during a hallmark period of development in which cortical volume peaks [9]. In prior studies, we utilized the dimensionless shape index to characterize cortical folding patterns across scales. Unlike curvature measures with specific units (e.g., mm^{-1} for mean curvature), the shape index is unitless, enabling direct comparisons of cortical shapes independent of size. Here, we employ a complementary metric, curvedness, to quantify the magnitude of cortical folding with respect to local shape. This metric allows us to describe the intensity of folding along the gyral-sulcal spectrum in relation to thickness changes, providing insight into cortical development during early infancy.

METHODS

In this study, we use longitudinal MRI data from 10 infants at 6, 12, and 24 months that were identified as 'at-risk' for Autism Spectrum Disorder (ASD) based on criteria from the National Database for Autism Research (NDAR). The segmentation process begins with cortical surface reconstructions derived from MRI scans. These images are processed using a deep learning pipeline developed by the BRAIN lab at UNC Medical School [10]. This pipeline addresses the challenge of distinguishing between white and gray matter in infant brains, where immature and unmyelinated neural tissue makes segmentation more difficult compared to adult brains.

From the segmented images the surfaces are reconstructed into triangular meshes, which are decimated and smoothed in preparation for computational analysis. Cortical thickness is calculated as the average distance between corresponding vertices on the pial and white surfaces, which are the upper and lower bound of the cortex, respectively. Our pipeline then computes classical metrics of cortical

folding, like Gaussian curvature, mean curvature, and sulcal depth at every vertex, alongside the unitless shape index, which classifies a continuous gradient of concave, saddle, and convex shapes [8]. Lastly, we introduce curvedness (CVD) into our pipeline, which possesses the unit of inverse length (1/mm, in this study). As shown in Fig. 1, shape index changes as the circumferential position around a circle of an axes of k_1 and k_2, the maximum and minimum curvatures at a point, where curvedness increases radially.

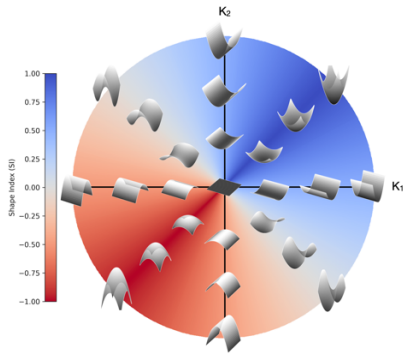

Figure 1: Surfaces plotted as a function of k_1 and k_2 in front of a Shape Index heatmap gradient.

RESULTS

Thickness and shape index distributions are shown in Fig. 2, noting a decrease in negative shape index values, typically sulcal in nature, with an increase in age and thickness.

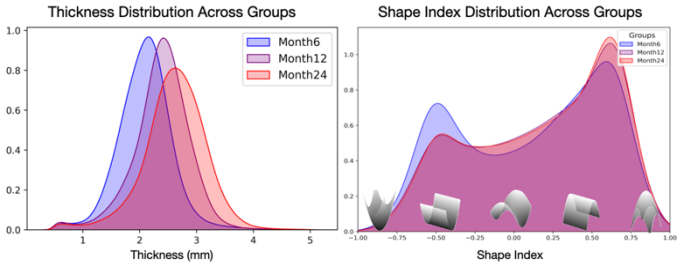

Figure 2: Thickness and Shape Index (SI) distributions across the three developmental ages.

We further segregate the data by SI category in Figure 3, depicting how the average thickness for shapes more sulcal in nature tend to increase and slightly "catch up" to shapes at lower curvedness values. Furthermore, a downwards-sloping, accelerated trend for the sulcal shapes implies that the most curved vertices thin more over time.

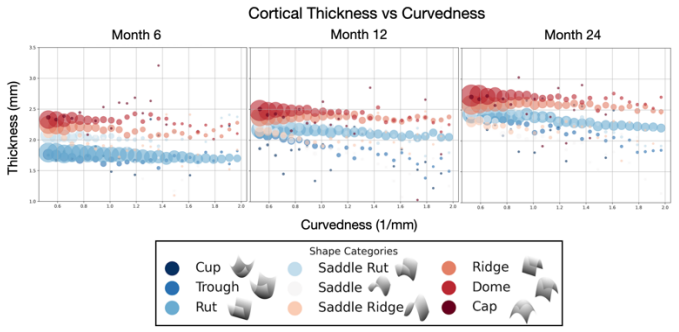

Figure 3: Density bubbles of thickness vs curvedness, segregated by SI category, shown across the three timepoints.

We also compared these distributions to adult subjects from our previous YALE dataset [8], which show similar curvedness distributions (Fig. 4). However, due to variations in segmentation toolboxes for the adult and infant groups, future studies will be required to compare thickness and curvedness changes across all ages.

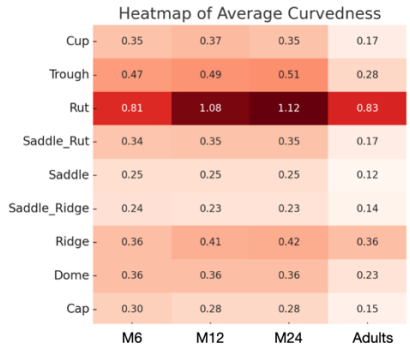

Figure 4: Heatmap of average curvedness values, separated by shape, for each age.

DISCUSSION

For the first time, curvedness was introduced as a complementary metric to shape index for a longitudinal cohort, enabling a more nuanced description of cortical morphology with unitless (SI) and scale-dependent (CVD) properties. This is suitable for a young, longitudinal cohorts experiencing relatively dramatic changes. Curvedness values markedly increased for sulcal shapes during the 6 and 12-month period, implying intensified sulcal definition, or deepening, while gyral regions displayed relatively static curvedness levels as they simultaneously increased in thickness. These results also set the stage for future investigations into atypical developmental trajectories, such as those associated with Autism Spectrum Disorder (ASD) like in this study, where personalized comparisons between subjects might shed light on expected development from childhood onward.

ACKNOWLEDGEMENTS

This work is supported by a CAREER grant from the National Science Foundation (CMMI-2144412). We thank Zhengwang Wu and Gang Li from the UNC Medical School's BRAIN lab for providing segmented infant MRI scans.

REFERENCES

[1] Klyachko VA et al. *Proc Natl Acad Sci USA.* 100:7937-7941, 2003.
[2] Wang X, Wang S, Holland MA. *Soft Matter*. 20:3053-3065, 2024.
[3] Wang S et al. *Biomech Model Mechanobiol*. 20:555-567, 2021.
[4] Holland, MA et al. *Phys Rev Lett*. 121: 228002, 2018.
[5] Darayi M et al. *J Biomech.* 139:110851, 2022.
[6] Demirci N et al. *NeuroImage*. 278:120283, 2023.
[7] Demirci N, Holland MA. *Cereb Cortex*. 34462, 2024.
[8] Demirci N, Holland MA. *Hum Brain Mapp*. 43:2064-2084, 2022.
[9] Bethlehem RAI et al. *Nature*. 604:525-533, 2022.
[10] Wang L et al. *Nature Protocols*. 18:1488-1509, 2023.